Formulation of hydrophobic peptides for skin delivery via coated microneedles

Authors: [1,2]Xin Zhao, [1]Sion A. Coulman, [2]Stephanie J. Hanna, [2]F. Susan Wong, [2]Colin M. Dayan and [1]James C. Birchall

Department: [1]School of Pharmacy and Pharmaceutical Sciences, Cardiff University, Cardiff, UK; [2]School of Medicine, Cardiff University, Cardiff, UK.

Corresponding author:
Dr Sion Coulman
School of Pharmacy and Pharmaceutical Sciences
Redwood Building
King Edward VII Avenue
Cardiff
CF10 3NB
UK

Tel: +44 29208776418; Email: coulmansa@cf.ac.uk

Running title:

Keywords: Microneedle, hydrophobic, formulation, coating, peptide

Abstract

Microneedles (MNs) have been investigated as a minimally-invasive delivery technology for a range of active pharmaceutical ingredients (APIs). Various formulations and methods for coating the surface of MNs with therapeutics have been proposed and exemplified, predominantly for hydrophilic drugs and particulates. The development of effective MN delivery formulations for hydrophobic drugs is more challenging with dosing restrictions and the use of organic solvents impacting on both the bioactivity and the kinetics of drug release. In this study we propose a novel formulation that is suitable for MN coating of hydrophobic auto-antigen peptides currently being investigated for antigen specific immunotherapy (ASI) of type 1 diabetes. The formulation, comprising three co-solvents (water, 2-methyl-2-butanol and acetic acid) and polyvinylalcohol 2000 (PVA2000) can dissolve both hydrophilic and hydrophobic peptide auto-antigens at relatively high, and clinically relevant, concentrations (25 mg/ml or 12.5 mg/ml). The drug:excipient ratio is restricted to 10:1 w/w to maximise dose whilst ensuring that the dry-coated payload does not significantly impact on MN skin penetration performance. The coating formulation and process does not adversely affect the biological activity of the peptide. The delivery efficiency of the coated peptide into skin is influenced by a number of parameters. Electropolishing the metal MN surface increases delivery efficiency from 2.0±1.0% to 59.9±6.7%. An increased mass of peptide formulation per needle, from 0.37 µg to 2 µg peptide dose, resulted in a thicker coating and a 20% reduction in the efficiency of skin delivery. Other important performance parameters for coated MNs include the role of excipients in assisting dissolution from the MNs, the intrinsic hydrophobicity of the peptide and the species of skin model used in laboratory studies. This study therefore both exemplifies the potential of a novel formulation for coating hydrophobic and hydrophilic peptides onto MN devices and provides new insight into the factors that influence delivery efficiency from coated MNs. Importantly, the results provide guidance for identifying critical attributes of the formulation, coating process and delivery device, that confer reproducible and effective delivery from coated MNs, and thus contribute to the requirements of the regulators appraising these devices.

1. Introduction

Microneedles (MNs) are sharp, needle-like structures with diameters and lengths generally in the micron range. These structures are used to penetrate the upper layer of the skin in a non-invasive and painless manner to enable intraepidermal, intradermal and transdermal delivery of pharmaceutical products, or extraction of biological material for bio-sensing applications. Documented approaches to drug delivery via MNs include (i) MN penetration of skin to enhance permeation of a topically applied formulation, (ii) injecting, or extracting, materials through hollow MN apertures, (iii) delivering materials contained within a dissolving/degradable needle substrate, or (iv) coating the material of interest onto the surface of the needle for subsequent delivery [1]. Of these approaches, coated MNs have attracted significant attention due to the simplicity of MN manufacture and the potential to create a device with an integrated formulation that is dry-coated, and thus more stable for labile biologics. Coated MNs have been used for the pre-clinical and, in some cases, clinical delivery of a range of materials including desmopressin [2], influenza vaccine [3], plasmid DNA [4], siRNA [5], lidocaine [6], parathyroid hormone [7], botulinum toxin [8], measles vaccine [9], insulin [10], M2e-TLR5 [11], and human growth hormone [12].

The pharmaceutical formulation and procedure for coating MNs are fundamental to the coated MN approach. Various coating formulations and coating devices have been developed and exemplified. Most commonly, aqueous coating solutions are used to create a uniform thin film of material on a metallic MN surface [4, 7, 13-15]. Whilst these studies have demonstrated the ability to coat hydrophilic drugs and particulates onto MNs, published reports of successful MN coating using hydrophobic materials are limited and typically describe low drug loading doses [15, 16]. Gill and Prausnitz, 2007 used an acetonitrile and ethanol solvent system to dissolve curcumin, as a model hydrophobic molecule, within polymer matrices (poly(lactic-co-glycolic acid) or polyvinylpyrrolidone (PVP) [15]. Ethanol has also been used as a co-solvent to prepare a Eudragit E 100 co-polymer and propylene glycol coating formulation that is able to accommodate minoxidil to treat hair loss [16]. In another study, the hydrophobic anti-inflammatory drug ketoprofen was encapsulated in a hydrogel mixture and delivered using coated MNs; however the delivery efficiency was not reported [17]. Given that more than 40% of newly developed drugs are hydrophobic [29, 30], further work is required to design and optimise formulations to ensure that MN delivery systems can be fully exploited for emerging drug entities in a diversity of therapeutic areas.

As an example of an emerging therapeutic, coated MNs have recently been studied for the delivery of peptide auto-antigens as an antigen specific immunotherapy (ASI) for type 1 diabetes [18]. In contrast to conventional vaccinations, which are designed to activate the immune system, this therapy aims to induce tolerance as a means to treat autoimmune disease [19, 20]. MNs are well suited to this application as targeting skin dendritic cells with auto-antigen in a minimally invasive

manner is more likely to mediate a tolerogenic, rather than inflammatory, immune response. The challenge of formulating such materials for MN delivery into skin not only relates to dosing capacity but also maintaining the bioactivity of the coated peptide, which may be affected by the solvents used in the coating formulation and the complex processes used to coat the MNs [13, 21]. In this specific case it will also be important to select excipients that do not stimulate a non-specific inflammatory response.

This study aims to develop an optimised formulation for the coating and delivery of hydrophobic auto-antigens from stainless steel MNs. In doing so, the study provides new and improved understanding of those critical parameters that influence delivery efficiency using coated MNs, such as the hydrophobicity of the drug cargo, the role of excipients, the impact of MN surface properties on coating and the influence of coating thickness on skin penetration and delivery.

2. Methods

2.1. Microneedle and microneedle applicator manufacture

Stainless MNs were fabricated and electropolished as described previously [18]. Briefly, MNs were cut from stainless steel sheets using wire electrical discharge machining (Cardiff School of Engineering, Cardiff, UK). The MNs were either used without further processing or following electropolishing using a method adapted from that described previously [22] and used in a previous study [18]. A bespoke MN holder and application device was manufactured from biocompatible acrylate polymer (e-Shell 200; EnvisionTEC, Gladbeck, Germany) at the Cardiff School of Engineering using additive manufacturing. The applicator was designed to facilitate simultaneous insertion of three planar rows of coated MNs.

2.2. Coating procedure for MNs

To coat MNs, 0.4 µl of the required formulation (equating to 10 µg peptide from a 25 mg/ml coating solution) was taken up in a 10 µl ultra long pipette tip using a 2.5 µl pipette. The tip was then carefully removed from the pipette without disturbing the liquid cargo [5] [18]. Peptide was then deposited onto an individual MN by brushing the aperture of the pipette tip perpendicularly and sequentially over the point of each needle under a microscope. Each needle was then left to briefly air dry in ambient conditions, leaving peptide residue on the needle surface. This was repeated for the required number of needles until the entire coating formulation had been extracted from the pipette tip and coated onto the MN surfaces.

2.3. Selecting solvents and excipients for coating peptides

Three peptides, which have relevance to type 1 diabetes in the non obese diabetic (NOD) mouse model of type 1 diabetes, with different hydrophobicities were used in the study: WE14 (WSRMDQLAKELTAE), a peptide of chromogranin A, m31 (YVRPLWVRME), a mimotope that stimulates highly diabetogenic CD4 T lymphocytes in the NOD mouse [23], and pro-insulin B9-23 (SHLVEALYLVCGERG) (GL Biochem, Shanghai, China). The solubility of these peptides was tested in water, acetic acid, tert-butanol and tert-amyl alcohol (Sigma-Aldrich, Gillingham, UK). After determining the best combination of solvents for all three peptides, 10 µg of peptide was further formulated with 1 µg of the following excipients to improve the MN coating efficiency and assist dissolution in the skin: poly vinyl alcohol MW2000 (PVA 2000), polyethylene glycol MW1450 (PEG 1450), pluronic 127 (PF127), pluronic 68 (PF68) or 2-hydroxypropyl-β-cyclodextrin (2HPβCD) (Sigma-Aldrich, Gillingham, UK).

2.4. Determining the solubility of peptides in a coating formulation

Peptides were prepared in a coating formulation at a concentration of 12.5 or 25 mg/ml to evaluate solubility within the solvent system. To do this, the peptide solution was centrifuged at 1000g for 10 minutes. The clarity of the solution was then inspected against a white light board and compared to de-ionised water and a PVA solution (2.5 and 1.25 mg/ml).

2.5. Evaluating the effect of MN coating formulation on m31 bioactivity

BDC-2.5-TCR-Tg.NOD mice were bred and maintained in a specific pathogen-free environment (Joint Biological Services Unit, Cardiff University, Cardiff, UK). All experimental procedures were carried out in accordance with UK Home Office project license regulations and following approval by the Ethical Review Committee at Cardiff University.

Mice were sacrificed in a sealed chamber filled with CO_2. The spleen was removed, dissociated using a glass homogenizer and cells were filtered through a 70 µm cell strainer into a 50 ml Falcon tube. Cells were then pelleted at 400g for 5 minutes, lysed with 900 µl of de-ionised water and immediately neutralized with 100 µl of x10 PBS. Recovered splenocytes were then filtered for a second time through a 70 µm cell strainer and resuspended in RPMI 1640 media supplemented with 5% FCS, 2 mM L-glutamine, 50 µM 2-mercaptoethanol and 1 U/ml penicillin/streptomycin (complete media) and finally kept on ice prior to use.

A coating formulation of m31 peptide was prepared (the finalised coating formulations for each of the peptides are shown in Table 4 in the Results section) and MNs were coated with 0.4 µl of coating

formulation. In order to evaluate whether the coating formulation and process influenced peptide bioactivity, m31 peptide (lyophilised powder) or m31 peptide recovered following MN coating was dissolved to a concentration of 0.2, 2 or 20 ng/ml in RPMI 1640 media supplemented with complete media. Splenocytes (300,000/well) were cultured in 96-well round bottom plates together with 100 µl of complete media, to which 100 µl of m31 solution was added to give a final concentration of 0.1, 1 or 10ng/ml respectively. The plates were incubated at 37°C with 5% CO_2 for 3 days. IFNγ concentration in the supernatant was then analysed using an IFNγ ELISA (Mouse IFN gamma ELISA Ready-SET-Go kit, eBioscience, Altrincham, UK). In order to detect IFNγ, purified Rat Anti-mouse IFNγ antibody was used as the primary antibody and biotin Rat Anti-Mouse IFNγ as the detection antibody. To detect the secondary antibody, horseradish peroxidase (HRP) was added and the colour developed using 3,3,5,5-Tetramethylbenzidine (TMB) substrate solution. Once conversion had taken place, the reaction was stopped by adding H_2SO_4 solution. Data was then acquired using a Multiwave plate reader (Thermo Scientific, Loughborough, UK) set at 450nm to obtain the OD (optical density) value.

2.6. Modifying the coating thickness

To characterise coating thickness, 1µg PVA 2000 and 10 µg WE14-5TAMRA were coated onto 5, 15 or 30 electropolished needles, i.e. the material was distributed over different numbers of MNs to vary the coating thickness per individual MN. The total mass coated onto MNs was 11µg, therefore the average mass over 5, 15 and 30 needles was considered to be 2.2µg/needle, 0.73µg/needle and 0.37µg/needle respectively.

2.6.1. Imaging MNs using Scanning Electron Microscopy (SEM) and 3D optical profiling

For SEM characterisation of MNs, both uncoated and coated, the MNs were mounted on 32 x 10 mm aluminium specimen stubs (Agar Scientific, Stansted, UK) using a small piece of a 12 mm adhesive carbon tab (Agar Scientific, Stansted, UK). Leit-C Conducting Carbon Cement (Agar Scientific, Stansted, UK) was used to secure the specimen. Mounted samples were then placed in an EMscope sputter coater under a low-pressure argon atmosphere and coated with gold (Agar Scientific, Stansted, UK) to improve surface conductivity and increase generation of secondary electrons, thereby improving signal/noise ratio. Samples were observed using a JEOL JSM-840A scanning electron microscope (JEOL, Tokyo, Japan) operating at 5kV with image capture using a SIS ADDAII Image Grabber with analysis software (Soft Imaging System GmbH, Munster, Germany). The coating thickness was further imaged using a Zeta 3D optical profiler (Zeta Instruments, San Jose, USA). The thickness of the coating was analysed in two ways using the optical profiler software: (i) the longitudinal coating thickness along the microneedle shaft, i.e. from the tip to the centre of the needle base and (ii) the latitudinal coating thickness at 10 different

positions across the width of the MN; 10 measurements at 10 μm intervals from 30 μm from the needle tip to 120 μm from the needle tip.

2.7. Skin delivery using coated MNs

The delivery efficiency of coated MNs was tested in both human and mouse skin. All human skin samples were obtained from female patients undergoing mastectomy or breast reduction surgery with informed patient consent and local ethical committee approval (South East Wales Ethics Committee Ref. 08/WSE03/55). Excised skin was transported from surgery to the laboratory and stored at -20˚C. Before experimentation, frozen skin was defrosted at room temperature in PBS and the subcutaneous fat was removed by blunt dissection. Skin was then stretched to approximately its normal tension on a cork dissection board. MNs coated with either WE14-5TAMRA or m31-5TAMRA were firmly pressed into human skin explants and held in place for 10 minutes before removal and subsequent analysis of the tissue and the MNs. To apply MNs *in vivo*, an NOD mouse was shaved near the neck area using clippers. MN arrays were then applied to the skin for 10 minutes, with the mouse under general anaesthetic.

2.8. Quantifying delivery efficiency of Peptide-5-TAMRA using UV-vis absorbance

The delivery efficiency of 5-TAMRA conjugated peptides was inferred by determining the mean loading dose that was achieved on peptide-coated MNs and subtracting the mass of peptide that remained on individual MNs after skin insertion. Quantification was achieved using UV-vis spectrometry (NanoVue Plus Spectrophotometer, GE Healthcare Life Sciences, Little Chalfont, UK), After skin insertion, MNs were immersed in 100 μl of 10 %v/v acetic acid in a sealed container and maintained at 2-8°C for 15 minutes. The absorbance of peptide-5TAMRA in the acetic acid solution was then measured at 559 nm using a NanoVue™ spectrophotometer (GE Healthcare Life Sciences, Little Chalfont, UK) and the concentration of the residual peptide on the MN calculated using a standard calibration curve. The peptide delivery efficiency was then calculated using the equation:

Delivery efficiency (DE) = (Average mass of MN coated peptide - Coated peptide mass after skin insertion) / Average mass of MN coated peptide x 100%

2.9. Peptide-5-TAMRA distribution in human skin explants

Following treatment, human skin was immersed in optical cutting temperature embedding matrix at room temperature and then snap frozen using a mixture of methanol and dry ice. Sections (10 μm thickness) were obtained using a Cryostat FSE (Thermo Scientific, Loughborough, UK) with the chamber temperature and the sample temperature set at -20˚C. Peptide-5-TAMRA distribution within skin sections was visualised using a fluorescence microscope (Leica DM IRB Microscope,

Leica Microsystems, Milton Keynes, UK) and images processed using ImageJ software (Rasband, W.S., ImageJ, U. S. National Institutes of Health, Bethesda, Maryland, USA, http://imagej.nih.gov/ij/, 1997-2016).

3. Results:

3.1 Development of a MN coating formulation suitable for hydrophobic peptides

3.1.1 Selection of solvents

The amino acid sequences and some physicochemical properties of the peptides used in this study are listed in Table 1. The solubility of these peptides in water is in the order WE14>m31>pro-insulin B9-23. Initial attempts to dissolve these peptides involved protonation of water using acetic acid. The pH of acetic acid solutions at concentrations of 1.9, 2.2 and 2.6 mol/L is 2.24, 2.21 and 2.17 respectively. Whilst all of these acetic acid solutions were able to dissolve WE14 at concentrations ranging from 10 to 25 mg/ml, neither m31 nor pro-insulin B9-23 peptides were soluble in acetic acid solution with concentrations above 10 mg/ml.

Table 1. Peptide properties. Peptide properties were generated using the genscript online resource, available at **https://www.genscript.com/ssl-bin/site2/peptide_calculation.cgi**

Peptide	Sequence	Charge	Isoelectric point	pH	Overall % of hydrophobic and hydrophilic amino acids
m31	YVRPLWVR ME	1	9.3	Basic	Hydrophobic: 60% Hydrophilic: 30% Neutral: 10%
WE14	WSRMDQLA KELTAE	-1	4.43	Acidic	Hydrophobic: 43% Hydrophilic: 36% Neutral: 21%
Pro-insulin B9-23	SHLVEALYL VCGERG	0	5.48	Neutral	Hydrophobic: 40% Hydrophilic: 27% Neutral: 33%

Alcohols were thereafter investigated as potential co-solvents. Tert-butanol and tert-amyl alcohol were selected as candidate co-solvents due to their relatively low vapour pressure (to prevent evaporation during coating resulting in changes to formulation concentration), aqueous miscibility (with the acetic acid solution) and melting point (for frozen storage of the coating formulation). Table 2. lists some key physical properties of these two alcohols (tert-butanol and tert-amyl alcohol) compared to water. Tert-amyl alcohol, containing an additional methyl group to tert-butanol, has a

lower solubility in water, lower melting point and lower vapour pressure (Table 2). Preliminary studies indicated that whilst tert-butanol was not able to dissolve m31 and pro-insulin B9-23 at a high peptide concentration (≥10mg/ml), tert-amyl alcohol dissolved these peptides at this concentration. Tert-amyl alcohol was therefore identified as an appropriate solvent for the development of coating formulations for hydrophobic peptides, whilst water or acetic acid was sufficient for the more hydrophilic WE14 peptide. Tert-amyl alcohol was miscible in 1.7-3.5 mol/L acetic acid/water mixtures at a volume ratio of 1:5 v:v, without visual observation of phase separation.

Table 2. Solvent physical properties. The physical properties of acetic acid, tert-butanol, tert-amyl alcohol and water. All the data were cited from **http://www.chemspider.com/**

Compound	Molecular weight g/mol	Miscibility in water g/l	Melting point ˚C	Boiling point ˚C	Vapour pressure kPa (at 20˚C)
Acetic acid	60.05	Miscible	16 to 17	118 to 119	1.5
Tert-butanol	74.12	Miscible	25	82 to 83	4.1
Tert-amyl alcohol	88.15	120	-9.1	101 to 103	1.6
Water	18	-	0	100	2.3

3.1.2 Selection of additional excipients

A range of additional excipients was explored to i) assist dissolution of the coated peptide from the MN surface following insertion into skin, and ii) confer stability to the coating formulation. A previous Phase I clinical study has demonstrated the safety profile of a dose of 10μg pro-insulin C19-A3 peptide [24], and therefore 10μg of auto-antigenic peptide was selected as an appropriate dose to coat onto each MN array. Five excipients, listed in Table 3, were tested individually to improve coating efficiency (peptide alone was not able to coat the needle with the current coating method). In order to minimise the reduction in drug coating capacity, 1μg of each excipient was used to provide a 1:10 w/w excipient:drug ratio.

Table 3. Excipients tested as components in the coating formulation to improve coating efficiency.

Excipients	Function	Properties
PVA (MW 2000)	Dispersant	Polymer
PEG (MW 1450)	Dispersant	Polymer
PF127	Nonionic Surfactant (high molecular weight)	Thermogel
PF68	Nonionic Surfactant (low molecular weight)	Thermogel
2HPβCD	Form inclusion complex	Sugar ring

The excipients listed in Table 3 were added to the acetic acid/tert-amyl alcohol/water ternary solvent system using the same excipient to peptide ratio: 1:10 w:w. Only m31 peptide was used in these studies based upon its intermediary hydrophobicity.

The delivery capabilities of these excipient formulations were then examined in human skin. Electropolished MN devices (30 needles) delivered up to 70% of the coated peptide dose from coated MN formulations (Fig.1). Formulations containing 2HPβCD or PVA excipients enabled more effective m31-5TAMRA release into the skin than PEG, PF127 and PF68. Downstream concerns about an increase in the peptide dissociation rate and the potential stimulation of a non-specific immune response by 2HPβCD resulted in the selection of PVA 2000 as the coating excipient of choice.

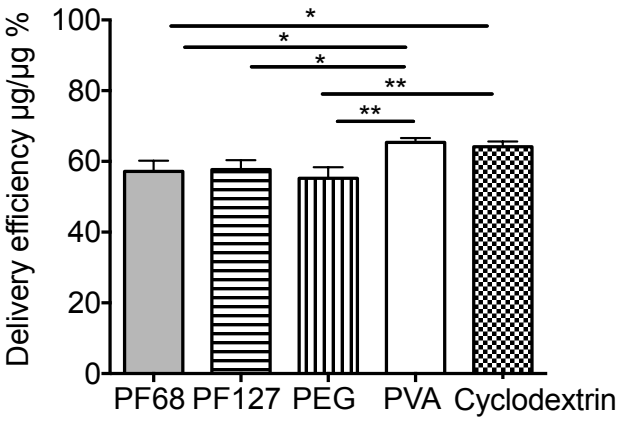

Fig.1. Effect of excipient selection on peptide delivery efficiency. Excipient effect on delivery efficiency of m31-5TAMRA using three arrays (30 needles) of electropolished 500µm MNs. MNs were coated with 10µg of m31-5TAMRA and applied to human skin explants for 10 minutes before analysing the delivery efficiency. N=3. Mean±SD. One-way ANOVA with Tukey's post test. *p<0.05, **p<0.01.

Table 4 summarises the composition of finalised formulations used to coat 10µg of the peptide in subsequent experiments.

Table 4. Coating formulation composition for each peptide. The formulation was tested for its ability to dissolve 1mg of each peptide. The range of excipients tested is listed in **Table 3.**

Peptide	Tert-amyl alcohol (v/v%)	Acetic acid Mol/L (v/v%)	Water (v/v%)	Peptide Conc. (mg/ml)	PVA Conc. (mg/ml)	Volume to coat 10µg peptide (µl)
m31	20	1.9 (11%)	69	25	2.5	0.4
WE14	-	2.6 (15%)	85	25	2.5	0.4
proinsulin B9-23	31.25	2.2 (12.5%)	56.25	12.5	1.25	0.8

3.1.3. Evaluation of bioactivity of a dry coated peptide formulation

To determine whether MN coating excipient (i.e. PVA 2000) or the dry coating processes affected the bioactivity of the m31 peptide (lyophilised powder), both the pure m31 (mimotope control) and the coated m31 peptide (recovered after MN coating) were cultured with splenocytes from BDC2.5-TCR-Tg mice (Fig.2). The bioactivity of m31 was determined by IFNγ release from BDC2.5 T cThere was no significant difference in the IFNγ production stimulated by control and coated m31 peptide at all studied concentrations (Fig.2). The negative control (Blank F), i.e. PVA 2000 solution alone, did not stimulate BDC2.5 splenocytes.

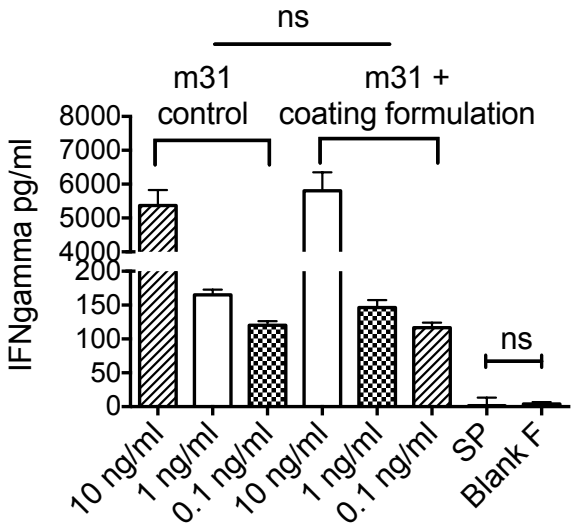

Fig 2. Effect of MN coating on peptide bioactivity. The bioactivity of m31 peptide after formulating and subsequent dry coating was compared to the pure unaltered m31 peptide (lyophilised powder). Three concentrations of m31 peptide (10, 1 and 0.1 ng/ml) were tested. Stimulation of the splenocytes by the peptide was determined by measuring IFNγ levels. SP=splenocytes alone. Blank F=blank formulation without adding m31 peptide. N=3, Mean±SD. Unpaired two-tailed t-test; ns p>0.05.

3.2. Understanding and optimising parameters that affect intradermal delivery of MN coated peptides

3.2.1. The influence of the MN surface morphology on MN coating and delivery of the peptide formulation

The surface morphology (roughness) of the MNs was modified by electropolishing (Fig. 3A). Visual observations of skin treated with m31-5TAMRA coated MNs indicated that unpolished MNs delivered less peptide than their electropolished counterparts (Fig.3B). This was confirmed quantitatively using UV-vis spectrometry (Fig.3C), where 59.9±6.7 % of the coated dose was delivered using electropolished 500µm MNs compared to 2.0±1.0 % from their unpolished equivalents.

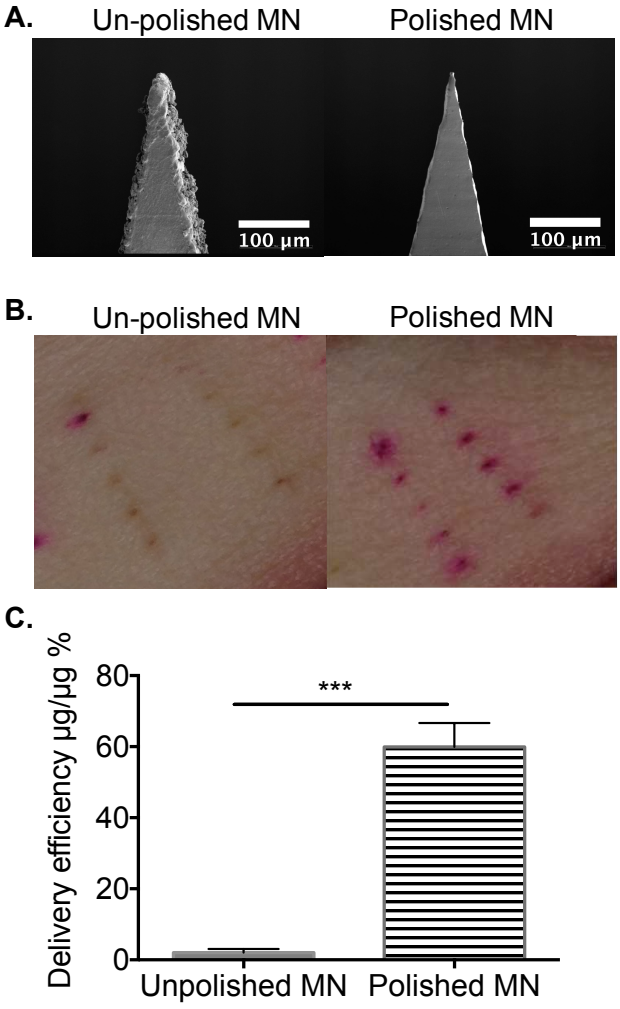

Fig.3. Effect of MN surface morphology/roughness on m31-5TAMRA delivery efficiency. A. SEM image of MN tip before (left) and after electropolishing (right). **B.** Images show MN array penetration and m31-5TAMRA (pink) release into human skin explants after a 10-minute application. MNs with different surface properties were coated with the same mass of peptide (10µg) and applied to the human skin explant for 10 minutes. The penetration images were visualised using a stereoscopic microscope and processed with ImageJ software. **C.** Effect of MN surface morphology/roughness on delivery efficiency in human skin explants. m31-5TAMRA was delivered using 500µm (30 needles) MNs with or without electropolishing. N=3. Mean±SD. One-way ANOVA with Tukey's post test. **p<0.01, ***p<0.001.

3.2.2. Characterising MN coating thickness

In order to better understand the distribution and thickness of the peptide formulation on the MN surface the coated MNs were imaged using SEM (Fig.4). Figure 4 shows that uncoated electropolished MNs have a smooth surface (Fig.4A) and an average needle length of 470.2 ± 13.4µm (Fig.4B). The optimised coating formulation and manual coating technique coated the MNs relatively reproducibly (Fig.4). The method ensured that the coating was focused on the upper portion of the MN i.e. 339.1±16.3µm (2.2µg/needle), 312.2±10.2µm (0.73µg/needle) and 309.8±19.6µm (0.37µg/needle) from the needle tip (Fig.4B). When the mass of the coated formulation was increased, the MN coating thickness increased whilst the distribution of the coating became less uniform i.e. it became concentrated in the central region of the needle (Fig.4 A, Fig.5, and Fig.6). This retained the tip sharpness. However, increasing the MN coating volume caused cracking of the dried film (Fig.4A; 2.2 and 0.73µg/needle). This was not observed on the thinly coated needles (Fig.4A; 0.37µg/needle). Nevertheless, the integrity of the coating remained intact during handling and microscopy of all of the coated MN arrays.

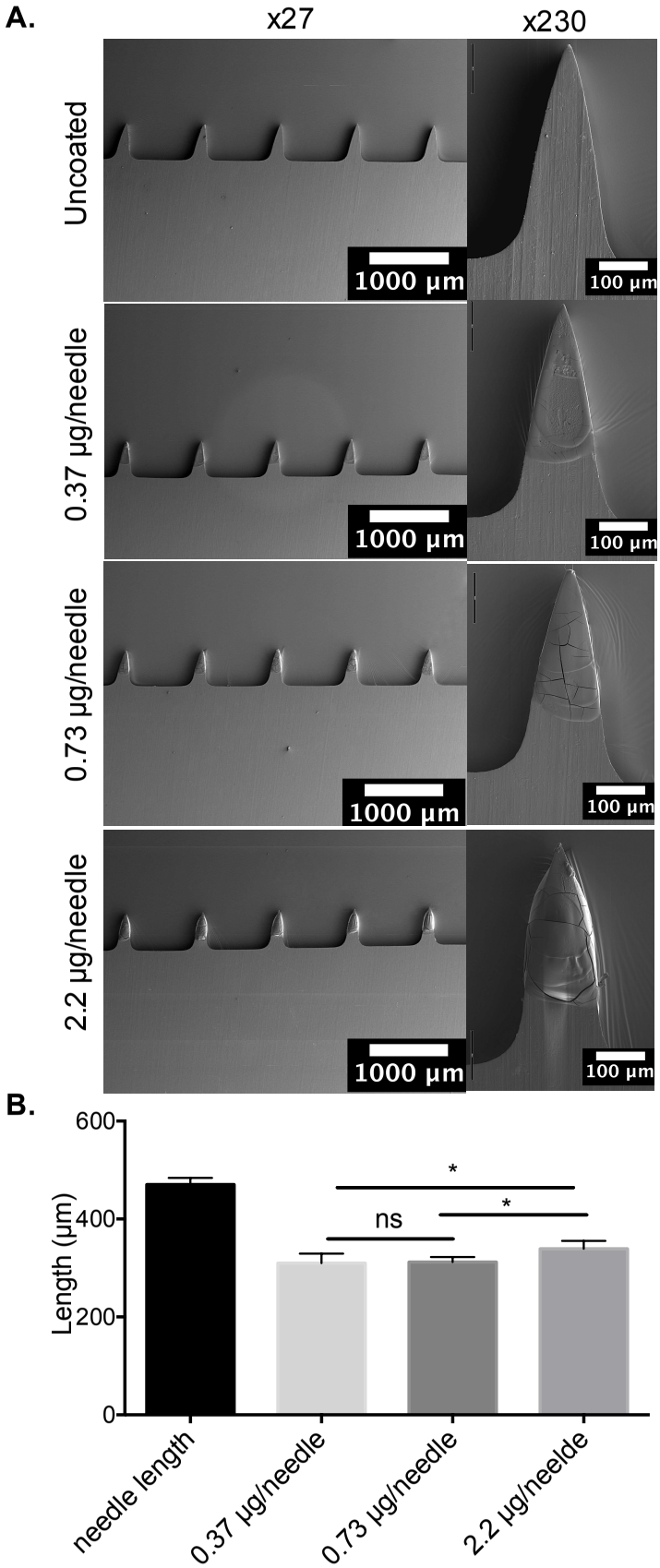
A.
x27
x230
Uncoated
0.37 µg/needle
0.73 µg/needle
2.2 µg/needle
1000 µm
100 µm
B.
Length (µm)
600
400
200
0
ns
*
*
needle length
0.37 µg/needle
0.73 µg/needle
2.2 µg/neelde

Fig.4. Coating distribution. A. SEM images of MNs coated with different coating doses. 10μg peptide and 1μg PVA were coated onto 5, 15 or 30 needles, producing concentrations of 0.37μg/needle, 0.73μg/needle and 2.2μg/needle. Uncoated and coated MNs were imaged at x27 and x230 magnifications. Scale bar: x27=1000μm, x230=100μm. B. Needle length and coating length. Coating length was measured from needle tip to the central coating base line. n≥5. One way ANOVA with Tukey post test, ns=$p>0.05$, *$p<0.05$.

The characteristics of the peptide coating were further analysed using a Zeta 3D optical profiler (Fig.5 and Fig.6), where coating thickness was analysed as a single longitudinal section (Fig.5) and in 10 latitudinal sections (Fig.6) taken from the microneedle tip to a position 120μm from the microneedle tip. Limited to the field of view of the instrument, the coating thickness was only measured on the upper 120μm of the MN. The height of the uncoated needle surface is evenly distributed across the 10 lines of latitude (Fig.6 A) and no change in surface height is observed along the longitude (Fig.5 A). Therefore the topography of uncoated microneedle surfaces is flat. When 30 individual needles were coated (notionally 0.37μg/needle) adhesion of the liquid formulation to the needle surface resulted in a fairly consistent coating thickness, changing by 1.1μm from the first (3.6±0.1μm) to the tenth (4.7±0.2μm) latitudinal cross section (Fig.6 B&E), which was also reflected in a near flat longitudinal cross section (Fig.5 B). When the formulation was coated over 15 individual needles (notionally 0.73μg/needle) the coating thickness varied from 0.10±0.08μm at 30μm from the MN tip to 4.20±0.122μm at a 120μm distance from the needle tip, a difference of 4.10μm (Fig.5 C, Fig.6 C&E). Latitude measurements of the thickest coating (5 needles i.e. theoretically 2.2μg of material per needle) indicated that the thickness of the coating changed from 1.09±0.50μm at the needle tip to 16.8±0.244μm at 120μm from the needle tip (Fig.6 D&E). This difference of 15.71μm was confirmed in the longitude gradient measurements (Fig.5 D).

Coating thickness also influenced the geometry of the coated MN. In the case of the thickest coating (2.2μg/needle), the coated MN assumed a more conical shape, as shown by the slope on the longitudinal thickness plot and the bell-shaped curves for latitudinal section plots (Fig 6. D). In the case of thinner coatings (both 0.73 and 0.37μg/needle), the slope of the longitudinal plots was less pronounced (note, the Y-axis 'thickness' scale was reduced when compared against the thickest coating plot) and the latitudinal cross section plots were generally flat (Fig.5 B&C). The cracks in the coating observed under SEM were also observed using the Zeta 3D profiler (Fig.5 D) and were evidenced by marked drops in surface height on the longitudinal thickness plot in the case of 2.2 μg/needle (Fig.5D; indicated by red arrows).

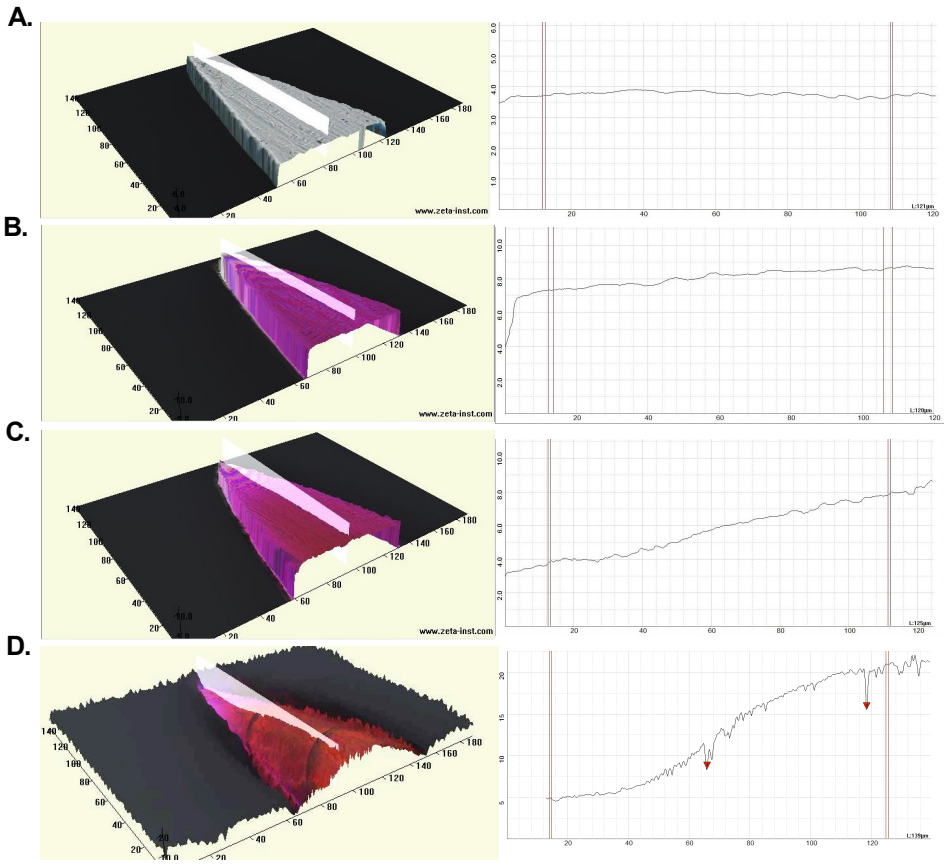

Fig.5. Longitudinal 3D optical profiling of the coating thickness of WE14-5TAMRA peptide. Change to the surface height was measured along the longitudinal axis of the needle, i.e. from the tip to the central region. Representative images and measurement of uncoated needle (A) and needles coated with 10µg peptide and 1µg PVA 2000 distributed over 30 (B), 15 (C) and 5 (D) needles producing concentrations of 0.37µg/needle (B), 0.73µg/needle (C) and 2.2µg/needle (D).

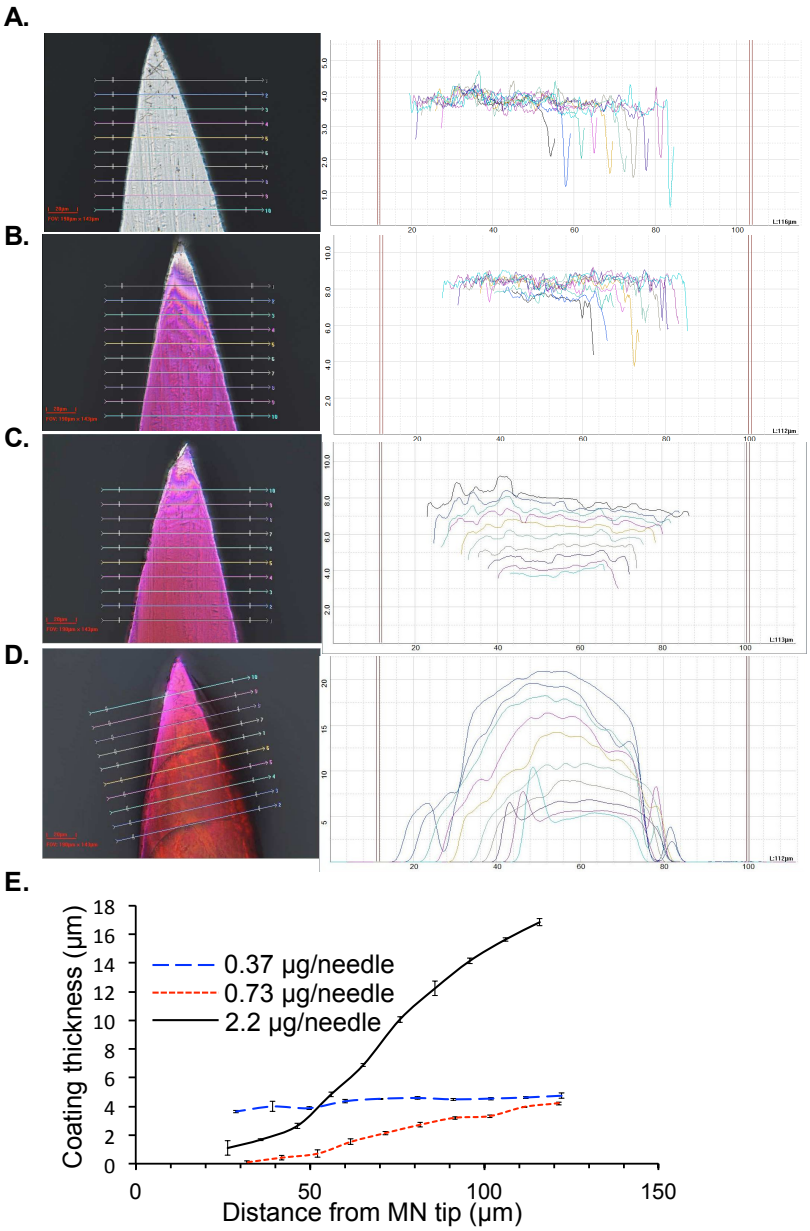

Fig.6. Latitudinal 3D optical profiling of the coating thickness of WE14-5TAMRA peptide. Changes to the surface height were measured at 10 different latitudinal locations from the MN tip to the central region. Representative images and measurement of uncoated needle (A) and needles coated with 10µg peptide and 1 µg PVA 2000 distributed over 30 (B), 15 (C) and 5 (D) needles producing concentrations of 0.37µg/needle (B), 0.73µg/needle (C) and 2.2µg/needle (D); E. Coating thickness of WE14-5TAMRA over the first 120µm from the needle tip for the 5, 15 and 30 needle samples producing mass loading of 0.37µg/needle, 0.73µg/needle and 2.2µg/needle. n=3.

3.2.3. Comparing the influence of coating thickness and peptide hydrophobicity on delivery efficiency in human and mouse skin

The delivery efficiency from coated MNs was compared in two skin models i.e. human skin explant and murine skin. For the hydrophilic peptide WE14-5TAMRA, the delivery efficiency from a 30 needle

MN array in the human skin explant was 90.4±1.9 %, whilst delivery efficiency in mouse skin was 60±6.6 % (Fig.7A, Table 5). For the hydrophobic peptide m31-5TAMRA, delivery efficiency from 30 MNs was reduced although still significantly higher in the human skin explant (58.9±3.2 %) than mouse skin (19.5±4.7 %) (Fig.7B, Table 5). This observation also translated to the thicker MN coatings, i.e. coating distributed over 15 or 5 needles (Fig.7A&B, Table 5).

The effect of coating thickness on delivery efficiency was also evaluated. For the hydrophilic peptide, WE14-5TAMRA, there was no difference in the delivery efficiency between 30 (90.4±1.9 %) and 15 (89.04±2.26 %) MNs when applied to human skin, whilst a significantly lower delivery efficiency was observed when using the thicker coating i.e. over 5 MNs (65.5±7.7 %) (Fig.7A, Table 5). In mouse skin, the delivery efficiency of WE14-5TAMRA also decreased significantly when coating thickness increased from 0.37μg/needle (30 MNs coated) to 2.2μg/needle (5 MNs coated) (Fig.7A, Table 5). For the hydrophobic peptide, m31-5TAMRA, there was no significant difference in the delivery efficiency when the coating was distributed over 30 MNs or 15 MNs, either in the human skin explant (58.9±3.2 % vs 50.6±8.0 %) or mouse skin (19.5±4.7 % vs 16.2±3.5 %) (Fig.7B, Table 5). However, when the dose was distributed over 5 needles i.e. thicker MN coatings, there was a significant reduction in the delivery efficiency in both human skin (38.6±1.7 %) and mouse skin (5.9±3.6 %) (Fig.7B, Table 5).

The intrinsic hydrophobicity of the peptide also influenced delivery efficiency when other parameters i.e. skin model and coating thickness, remained constant. Data in Fig.7C, relating to the use of 30 MNs for peptide delivery into the human skin explant, suggests a significant increase in delivery efficiency from the MN with an increasing aqueous solubility of the peptide i.e. insulin B9-23 (46.5±5.0 %) < m31 (58.9 ±3.2 %) < WE14 (90.4±1.9 %). Distribution of the m31 and WE14 peptides also differed in human skin. Whilst m31 peptide was delivered proximal to the microchannel created by the MN devices, WE14 peptide was more widely distributed in the epidermis and dermis following application of the coated MN to human skin (Fig.7D).

Table 5. Delivery efficiency of WE14-5TAMRA and m31-5TAMRA in mouse skin and human skin explant. Data presented as Mean±SD % H=human skin explant, M=mouse skin

Needle number	Coating thickness μg/needle	Skin Model	Peptides	
			WE14-5TAMRA	m31-5TAMRA
30	0.37	H	90.38±1.94 %	58.9±3.2 %
		M	60.0±3.9 %	19.5±4.7 %

15	0.73	H	89.04±2.26 %	50.6±8.0 %
		M	44.8±8.8 %	16.2±3.5 %
5	2.2	H	65.48±7.66 %	38.6±1.7 %
		M	23.5±3.4 %	5.9±3.6 %

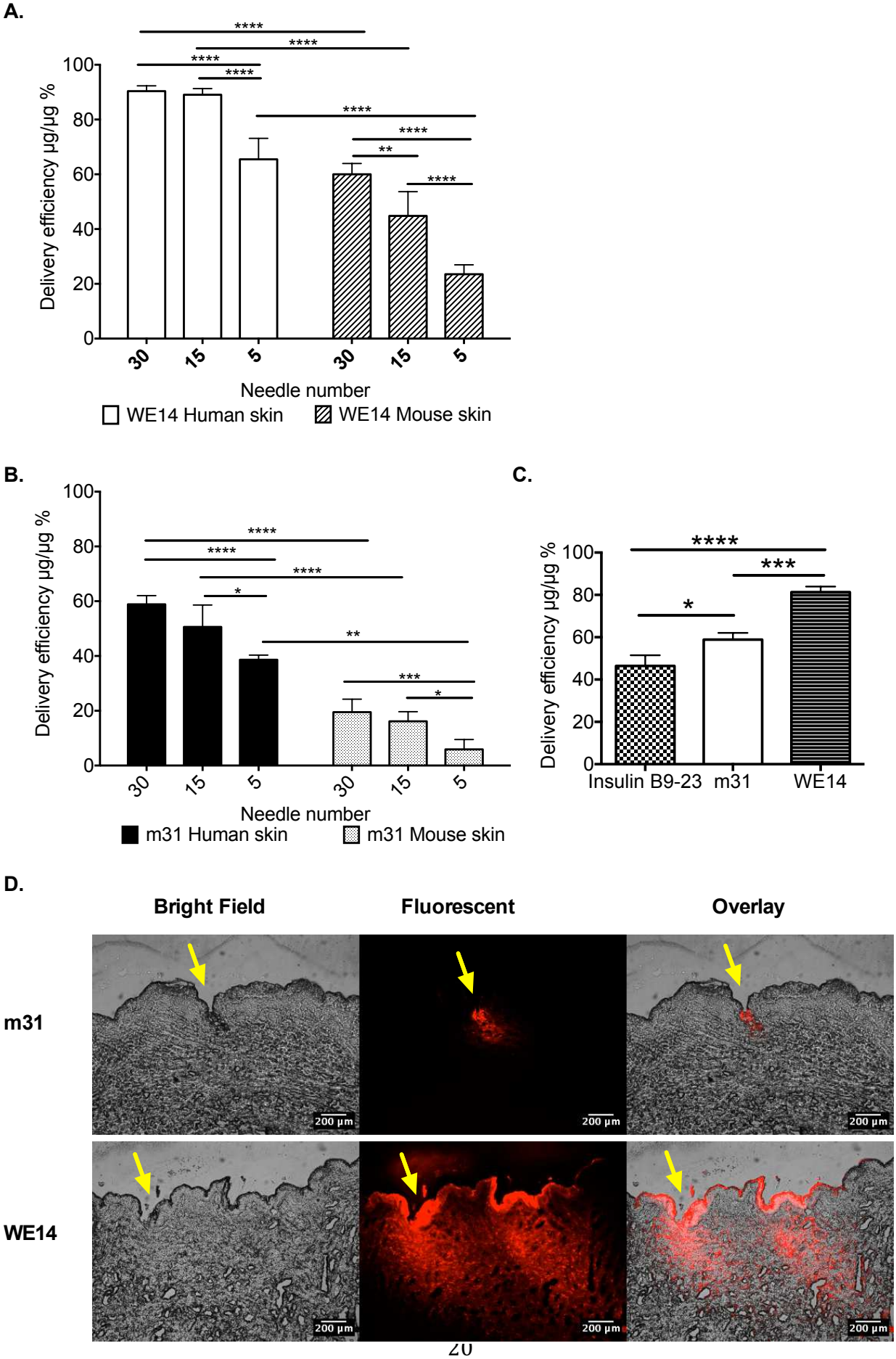
A.
Delivery efficiency µg/µg %
100
80
60
40
20
0
****
****
****
****
****
**
****
30
15
5
30
15
5
Needle number
WE14 Human skin
WE14 Mouse skin
B.
Delivery efficiency µg/µg %
100
80
60
40
20
0
****
****
****
*
**
***
*
30
15
5
30
15
5
Needle number
m31 Human skin
m31 Mouse skin
C.
Delivery efficiency µg/µg %
100
80
60
40
20
0
****
***
*
Insulin B9-23
m31
WE14
D.
Bright Field
Fluorescent
Overlay
m31
WE14
200 µm

Fig.7. Comparing the influence of coating thickness and peptide hydrophobicity on delivery efficiency in human and murine skin. Electropolished MNs with different needle numbers (5, 10 or 30) were coated with 10µg of peptide-5TAMRA. Delivery efficiency of m31-5TAMRA was quantified after 10 minutes application either in human skin explant or in mouse skin. A. Effect of skin derivation and coating thickness on delivery efficiency of WE14-5TAMRA. B. Effect of skin derivation and coating thickness on delivery efficiency of m31-5TAMRA C. Effect of peptide hydrophobicity on delivery efficiency in human skin explants using electropolished 500µm MNs. The same mass (10µg) of hydrophilic peptide, WE14, and hydrophobic peptide (m31 and proinsulin B9-23) was coated and delivered to human skin explants using 3 arrays of ten 500µm long electropolished MNs. Delivery efficiency was then calculated after MN application. Statistics for Fig.7A, B and C: n≥3. Mean±SD, one way ANOVA with Tukey post test, *p<0.05, **p<0.01, ***p<0.001, ****p<0.0001. D. Distribution of peptide-5TAMRA in human skin explant. Human skin explant was treated with 30 MNs coated with WE14-5TAMRA or m31-5TAMRA. Scale bar=200µm.

4. Discussion

4.1. Developing a coating formulation for hydrophobic peptides

Several formulations have been developed previously for coating MNs including a coating formulation developed at GeorgiaTech, which was used to coat peptide, vaccine, salmon calcitonin, bovine serum albumin and plasmid DNA [13, 15, 21, 22, 25]. This aqueous formulation typically contains 1% (w/v) carboxymethylcellulose sodium salt, 0.5 % (w/v) Lutrol F-68 NF and 15 % (w/v) trehalose in PBS. If a poorly soluble hydrophobic peptide were able to dissolve in this coating formulation at a concentration of 1mg/ml, i.e. 0.1 % (w/v), then the API to excipient ratio would be 1:165, i.e. 1650µg of excipient would be co-coated with the target dose of 10µg of peptide. The mass of excipients required in this scenario would therefore be prohibitive for some MN applications. Coating formulations designed for more hydrophobic molecules have also been reported, although these studies are more limited. Gill et al. utilised organic solvents such as ethanol and acetonitrile to dissolve hydrophobic compounds for MN coating [15]. One disadvantage of these solvents is their high volatility. This makes it difficult to control the coating formulation concentration, which can influence the accuracy and repeatability of coating. The authors also investigated a coating formulation for hydrophobic molecules using a molten polymer, polyethylene glycol (Molecular Weight 1500). However, the high process temperature (45˚C) and the low drug loading capacity (0.01%w/v) make this impractical for biologics. The present study describes a coating formulation suitable for three hydrophobic peptides, WE14, m31 and proinsulin B9-23 which have potential clinical applications for ASI for T1D.

A number of critical parameters were identified as key to the suitability of a MN coating formulation for therapeutic hydrophobic peptides: (i) a predominantly aqueous system that maintains peptide bioactivity, (ii) co-solvents to be, at least partially, miscible with water and have a similar vaporisation rate, in order to prevent phase separation, (iii) formulation evaporation at room temperature and atmospheric pressure to allow peptide coating and MN drying using ambient conditions, (iv) excipients that do not stimulate a pro-inflammatory immune response, (v) a minimal excipient mass

to maximise the peptide loading capacity of the MN, without reducing tip sharpness, (vi) peptide solubility of ≥ 10mg/ml to minimise the volume of coating formulation required and hence the coating time, and (vii) formulation stability at -80 ˚C to enable long term storage of peptide with maintained bioactivity, (vii) lack of toxicity toward the targeted responding cells.

The first step to develop a formulation to meet these criteria was to use a pH modifier to increase peptide polarity and solubility. Acetic acid is a weak organic acid that has been widely used to dissolve hydrophobic peptides [26] and insulin [27]. A 2M aqueous acetic acid solution can be used to dissolve WE14, a peptide with 43% hydrophobic groups, at a concentration of 25mg/ml. However, for other hydrophobic peptides such as m31, a basic peptide with 60% hydrophobic groups, and proinsulin B9-23, a neutral peptide containing 40% hydrophobic groups, increasing ionisation alone was not sufficient to ensure dissolution at the desired concentration and therefore a co-solvent was also included. DMSO (dimethyl sulfoxide) is a commonly used solvent for dissolving hydrophobic peptides. However the formation of sulphoxide or disulphide bonds with amino acids, such as cysteine, methionine and tryptophan residues [28] make it inappropriate for the methionine and tryptophan containing WE14 and m31. Alcohols were considered to be more appropriate co-solvents with a focus on a carbon chain length of below 5 to ensure that the hydrophilic influence of the hydroxyl group was not compromised by the hydrophobic effects of the hydrocarbon chain. Two alcohols were selected, tert-butanol and tert-amyl alcohol. Tert-butanol was unable to dissolve peptide at the desired concentration, even with the addition of acetic acid solution. However, tert-amyl alcohol was able to dissolve m31 at a concentration of 50mg/ml and proinsulin B9-23 at 25mg/ml. As tert-amyl alcohol is known to be only partially miscible with water it was necessary to test the miscibility of the ternary system i.e. water, acetic acid and tert-amyl alcohol. The ternary system was able to form a uniform mixture when the respective molar ratios fell beneath the solubility ternary phase curve [29] and therefore tert-amyl alcohol proved to be an appropriate co-solvent in the coating formulation.

Five additional excipients that were able to modify the surface tension of the coating formulation were also assessed to optimise adhesion of the coating to the MN whilst enabling de-coating *in situ.* The addition of the dispersant PVA 2000 was shown to provide both effective MN coating and effective delivery of the coated formulation into human skin, possibly because PVA 2000 dissolves more rapidly in an aqueous environment than other excipients, resulting in rapid release of the peptide into the skin. Results of the splenocyte stimulation experiment (IFNγ readout) indicated that the concentration of PVA 2000 used in the coating formulation did not trigger a non-specific inflammatory response. This is an important requirement when the goal is to induce immune tolerance rather than activation [18]. PVA 2000 was therefore included as an excipient (stabiliser, viscosity enhancer, dispersant) in the coating formulation. During formulation of the coating solution

the tert-amyl alcohol, acetic acid solution and PVA solution were added sequentially to the peptide to ensure complete peptide dissolution. Deviation from this resulted in insufficient dissolution of hydrophobic peptides. This is possibly because tert-amyl alcohol acts as dispersant increasing the contact area with the acetic acid, which then protonates the free peptide and increases its aqueous solubility.

This novel combination of excipients enabled coating of even the most hydrophobic peptides without a significant and detrimental effect on the MN dosing capacity i.e. only 1μg of excipient was coated onto the MN array for every 10μg peptide. This excipient:drug ratio is considerably lower than ratios reported in other studies using hydrophobic compounds [15] or peptides [21]. This is accompanied by preserved bioactivity of the peptide, as illustrated by the stimulation of IFNγ production by the m31 peptide, also shown in a previous publication which used WE14 and EBVP1 peptides [18], and a formulation that would potentially be considered biocompatible. Evaporation of the volatile co-solvents and the use of an approved pharmaceutical excipient, PVA, which is available as a clinical grade material, would allow the coating formulation to potentially be translated to clinical use. This stated formulation therefore provides encouragement to those developing dry coated MN systems for the clinical delivery of hydrophobic biologics.

4.2. Optimising delivery from coated stainless steel MNs

Effective localised delivery of a therapeutic cargo from a coated MN that has been inserted into human skin relies upon release of the peptide from the MN surface. Subsequent peptide dissolution and diffusion then controls local pharmacokinetics. The combined effect of these processes contributes to the final delivered dose. Stainless steel MN arrays were electropolished in-house to determine the influence of the gross MN surface morphology on peptide release *in situ*. Electropolishing reduced MN dimensions by approximately 12.5% and therefore, during the design of electropolished MN delivery systems, this reduction in needle height must be accounted for. Whilst the m31-5TAMRA peptide was not released from unpolished MNs in the local skin environment, electropolished MNs released approximately 60% of the peptide from the MN surface. Therefore, whilst the reduced surface roughness of the electropolished MN maintains efficient coating, it also minimises adherence of the coating material to the needle surface and thus facilitates more effective delivery of the payload on insertion/removal of the MN. The surface features of MNs, at the micron scale, may therefore be important parameters in the design of coated MN drug delivery systems.

The MN coating thickness was analysed by SEM and a Zeta 3D optical profiler. Observations using SEM suggested that the manual coating process is able to create reproducible coating thicknesses with a very small standard deviation. The coating length covered 65-70% of the needle length from

the tip and the base of the MN remained uncoated. When 10µg of WE14-5TAMRA was distributed over 5 needles (2.2µg/needle) the coating length was significantly greater than thinner coatings (0.37 and 0.73µg/needle). Previous studies indicate that the full length of the MN is not inserted into the skin (Sup Fig1 and [30, 31]) and therefore a difference in the length of the coating becomes more important if a proportion of the coated area of MN is not inserted into the tissue. In the development of coated MNs delivery systems for clinical use it will therefore be important to develop a coating formulation, and process, that ensures reproducible coating of the needle shaft to a length that is appropriate for the insertion characteristics of the specific MN device and/or applicator system.

On further inspection, SEM images revealed cracks in the dried formulation on the more thickly coated MNs (0.73 and 2.2 µg/needle) but not on those with the thinnest coating (0.37µg/needle). The Zeta 3D profiler also identified such cracks, confirming that these features are not simply a result of sample processing for SEM, but rather a result of volume contraction during the evaporative drying process under ambient conditions. Data from delivery efficiency experiments indicate that surface cracks do not significantly affect delivery and no obvious deleterious effects were witnessed during laboratory handling. However, the integrity of the dry-coated formulation should be considered in the handling, transport and storage of dry coated MNs when translating the technology to mass and widespread clinical utility. The Zeta 3D profiler was also used to measure the thickness of the MN coating. The tips of needles were shown to remain sharp in all three cases, with only slight changes (1-4 µm) to the width of the uncoated needle tip. Where 2.2µg of coating material is loaded per needle, the thickness of the coating film increases significantly at a distance of 40µm from the needle tip. The change in coating thickness was less dramatic when the coating was distributed over 15 needles (0.73µg/needle). A more uniform coating thickness was achieved when the 11µg of coated material (10µg peptide plus 1µg excipient) was distributed over 30 individual MNs. Therefore, when thinner coatings are applied, surface adhesion results in even distribution of the coated material. However, when thicker coatings are employed surface tension and cohesive effects draw the coating formulation towards the centre of the needle and way from the needle tip resulting in less coating at the very tip of the needle and accumulation of the coating towards the centre of the needle. This is clearly evident when 2.2µg of material is loaded per needle as both the longitudinal and latitudinal measurements show that the coating thickness rapidly overtakes the thickness of the thinnest coating even towards the very tip of the needle. Whilst the thickness of the 0.73µg/needle coating does not overtake the (consistent) thickness of the 0.37µg/needle coating up to 120µm from the tip of the needle, the increasing trajectory of coating thickness suggests that it will towards the centre of the needle. Controlling and validating the coating of MNs will became increasingly important as MN devices move from the laboratory bench to clinical trials and industrial manufacture. In this study, the Zeta 3D profiler has proved to be a useful tool for analysing transparent or semi-transparent MN coatings and could be used as a rapid screening quality control tool.

Differences in the uniformity of coatings may not only be a process control issue but may also translate to differences in skin delivery efficiency, causing heterogeneity in the dissolution of the coating from a MN and into the surrounding skin environment. Uniform coating is likely to facilitate more uniform release and dissolution from the MN surface, thus improving delivery efficiency and consistency. This may be particularly important when materials of reduced aqueous solubility are coated. Cormier et al., 2004 [2] demonstrated that an increased coating thickness resulted in reduced delivery efficiency when an increased mass of desmopressin was coated on steel MNs. In this study we show that when 10µg of a relatively hydrophobic peptide, m31-TAMRA, was distributed over 15 needles, rather than just 5 needles, resulting in a thinner coating, the delivery efficiency is dramatically increased. Delivery efficiency was further increased when the m31-TAMRA formulation was coated over 30 needles although this was not statistically significant.

Peptide hydrophobicity may be expected to influence delivery efficiency when coated MNs are inserted into skin. This study used excised human skin to confirm that more hydrophilic peptides (WE14) can be delivered more efficiently than more hydrophobic peptides (m31 and proinsulin B9-23). Traditional topical transdermal drug delivery tends to favour drugs that are hydrophobic, however the electropolished coated MNs used in this study circumvents the lipophilic SC barrier and introduces the therapeutic peptide to a depth of 300-400µm below the skin surface (Sup Fig.1). This targets the payload to the viable epidermis and papillary dermis. The dermis is an aqueous region of tissue, consisting of 70% water [32] and therefore improved delivery of a more hydrophilic peptide may be facilitated by more rapid and extensive dissolution in the local tissue.

Disease models are required to test the biological functionality of most novel pharmaceuticals and therefore delivery efficiency from the coated MN was also examined in mouse skin. There are notable biomechanical, architectural and biological differences between human and mouse skin [33-35] and these differences translated to differences in the delivery efficiency witnessed in this study for both the hydrophilic WE14 peptide and the more hydrophobic m31 peptide. In all of the studied conditions, delivery efficiency in mouse skin was significantly less than in human skin. We postulate that this reduced delivery efficiency is a direct result of differences in the dimensions of the tissue and the water available for dissolution. The thickness of human epidermis is typically 60-100µm compared to 20µm in mouse skin ([36, 37] and sup Fig.2), and the human dermis is 1.6-2.6mm [38] compared to just 200-300µm in the mouse. The absolute water content available for dissolution of the MN coating is therefore considerably less in the mouse model and results in a significantly reduced delivery efficiency compared to its human counterpart. With this in mind, when testing coated MN devices, it is important to consider both the source of the skin and its level of hydration.

Although the dermis is a hydrated aqueous environment, the free water available for dissolution of the MN coating in the tissue proximal to the inserted needle is finite [39]. This, together with the previously discussed coating thickness and aqueous solubility of the peptide, determines the saturation threshold for the MN delivered peptide. Therefore the most hydrophilic peptide tested, (WE14), dissolves readily in human skin tissue with no significant difference in delivery to human skin efficiency when the dose is coated over 30 needles compared to 15 needles. It is only when the thickness is significantly increased, with the drug coated over just 5 needles, that delivery efficiency in human skin is significantly reduced. This has also been witnessed for other water-soluble drugs delivered by coated MNs. For example, low dose and high dose (1μg or 7μg) bevacizumab, coated MNs can achieve similar delivery efficiency between 40%-50%, albeit in an ocular study [40]. Similar observations were also made for human growth hormone coated MNs delivered into skin [12]. For less soluble drugs, such as the m31 peptide, there is likely to be local saturation. This may necessitate extended insertion times to enable complete dissolution of the MN coating. However, this study has shown that it is possible to negate this saturation effect by distributing the dose over a greater number of MNs, thus enabling thinner MN coatings and smaller localised doses of drugs that are targeted to a wider area of the tissue. The number of individual MNs on an array is a modifiable parameter that can therefore be optimised for the specific drug to facilitate efficient and rapid drug release whilst maintaining the total delivered dose. However, it should be noted that changes to MN numbers and/or arrangements to accommodate different active pharmaceutical ingredients is also likely to influence the penetration performance of the device and this must be considered by MN developers during the pre-clinical phase.

5. Conclusion

In conclusion, a novel MN coating formulation system was developed for coating peptides with a spectrum of aqueous solubility. This formulation contains ternary co-solvents, water, 2-methyl-2-butanol (amyl-alcohol) and acetic acid, and PVA 2000. No loss of bioactivity was detected when peptides were formulated using this coating solution and the peptides could be reproducibly delivered to skin from the surface of electropolished MNs.

The factors influencing the cutaneous delivery efficiency of peptides from coated MNs include: 1) choice of excipient, 2) intrinsic hydrophobic property of the chosen peptide, 3) surface morphology/roughness of the MNs, 4) the coating thickness and 5) the species of skin model. This provides useful guidance in identifying critical attributes of the formulation, coating and delivery process that confer reproducible and effective delivery of coated MN formulations and contributes to the requirements of the regulators appraising these devices.

We propose a general formula showing the relationship between some of the critical factors that influence the delivery efficiency of coated MNs:

$$DE \propto \frac{1}{Hydrophobicity}, \frac{1}{Roughness}, \frac{N}{Mass}, H$$

DE = Delivery efficiency
$\propto$ = Proportional to
Hydrophobicity = Hydrophobicity of coated API
Roughness = MN surface roughness
Mass = Total mass coated onto MNs
N = Total number of MNs
H = Hydration state of the skin

Whilst we acknowledge that formulation excipients also play an important role in the delivery efficiency from a coated MN, in this study only a small proportion of excipient was employed and therefore its impact on delivery efficiency was minimised.

References:

[1] Y.C. Kim, J.H. Park, M.R. Prausnitz, Microneedles for drug and vaccine delivery, Adv Drug Deliv Rev, 64 (2012) 1547-1568.
[2] M. Cormier, B. Johnson, M. Ameri, K. Nyam, L. Libiran, D.D. Zhang, P. Daddona, Transdermal delivery of desmopressin using a coated microneedle array patch system, Journal of Controlled Release, 97 (2004) 503-511.
[3] Y.C. Kim, F.S. Quan, R.W. Compans, S.M. Kang, M.R. Prausnitz, Stability kinetics of influenza vaccine coated onto microneedles during drying and storage, Pharm Res, 28 (2011) 135-144.
[4] M. Pearton, V. Saller, S.A. Coulman, C. Gateley, A.V. Anstey, V. Zarnitsyn, J.C. Birchall, Microneedle delivery of plasmid DNA to living human skin: Formulation coating, skin insertion and gene expression, Journal of Controlled Release, 160 (2012) 561-569.
[5] R.H.E. Chong, E. Gonzalez-Gonzalez, M.F. Lara, T.J. Speaker, C.H. Contag, R.L. Kaspar, S.A. Coulman, R. Hargest, J.C. Birchall, Gene silencing following siRNA delivery to skin via coated steel microneedles: In vitro and in vivo proof-of-concept, Journal of Controlled Release, 166 (2013) 211-219.
[6] Y. Zhang, K. Brown, K. Siebenaler, A. Determan, D. Dohmeier, K. Hansen, Development of lidocaine-coated microneedle product for rapid, safe, and prolonged local analgesic action, Pharm Res, 29 (2012) 170-177.
[7] M. Ameri, S.C. Fan, Y.F. Maa, Parathyroid hormone PTH(1-34) formulation that enables uniform coating on a novel transdermal microprojection delivery system, Pharm Res, 27 (2010) 303-313.
[8] B.M. Torrisi, V. Zarnitsyn, M.R. Prausnitz, A. Anstey, C. Gateley, J.C. Birchall, S.A. Coulman, Pocketed microneedles for rapid delivery of a liquid-state botulinum toxin A formulation into human skin, Journal of Controlled Release, 165 (2013) 146-152.
[9] C. Edens, M.L. Collins, J. Ayers, P.A. Rota, M.R. Prausnitz, Measles vaccination using a microneedle patch, Vaccine, 31 (2013) 3403-3409.
[10] S. Xie, Z. Li, Z. Yu, Microneedles for transdermal delivery of insulin, Journal of Drug Delivery Science and Technology, 28 (2015) 11-17.
[11] B.Z. Wang, H.S. Gill, C. He, C. Ou, L. Wang, Y.C. Wang, H. Feng, H. Zhang, M.R. Prausnitz, R.W. Compans, Microneedle delivery of an M2e-TLR5 ligand fusion protein to skin confers broadly cross-protective influenza immunity, J Control Release, 178 (2014) 1-7.
[12] M. Ameri, M. Kadkhodayan, J. Nguyen, J.A. Bravo, R. Su, K. Chan, A. Samiee, P.E. Daddona, Human Growth Hormone Delivery with a Microneedle Transdermal System: Preclinical Formulation, Stability, Delivery and PK of Therapeutically Relevant Doses, Pharmaceutics, 6 (2014) 220-234.
[13] Y.C. Kim, F.S. Quan, R.W. Compans, S.M. Kang, M.R. Prausnitz, Formulation and coating of microneedles with inactivated influenza virus to improve vaccine stability and immunogenicity, J Control Release, 142 (2010) 187-195.
[14] S. Ross, N. Scoutaris, D. Lamprou, D. Mallinson, D. Douroumis, Inkjet printing of insulin microneedles for transdermal delivery, Drug Deliv Transl Res, 5 (2015) 451-461.
[15] H.S. Gill, M.R. Prausnitz, Coating formulations for microneedles, Pharm Res, 24 (2007) 1369-1380.
[16] A.G.P. Namrata B. Date, Dr. Smita S. Pimple, Dr. Pravin D. Chaudhari, formulation and evaluation of coated microneedles for the treatment of hairloss, IJRRPAS, 4 (2014) 1083-1101.
[17] J.W. So, H.H. Park, S.S. Lee, D.C. Kim, S.C. Shin, C.W. Cho, Effect of microneedle on the pharmacokinetics of ketoprofen from its transdermal formulations, Drug Deliv, 16 (2009) 52-56.

[18] X. Zhao, J.C. Birchall, S.A. Coulman, D. Tatovic, R.K. Singh, L. Wen, F. S. Wong, C.M. Dayan, S.J. Hanna, Microneedle delivery of autoantigen for immunotherapy in type 1 diabetes, Journal of Controlled Release, 223 (2016) 178-187.
[19] M. Peakman, M. von Herrath, Antigen-specific immunotherapy for type 1 diabetes: maximizing the potential, Diabetes, 59 (2010) 2087-2093.
[20] C.A. Sabatos-Peyton, J. Verhagen, D.C. Wraith, Antigen-specific immunotherapy of autoimmune and allergic diseases, Curr Opin Immunol, 22 (2010) 609-615.
[21] C. Tas, S. Mansoor, H. Kalluri, V.G. Zarnitsyn, S.O. Choi, A.K. Banga, M.R. Prausnitz, Delivery of salmon calcitonin using a microneedle patch, Int J Pharm, 423 (2012) 257-263.
[22] H.S. Gill, M.R. Prausnitz, Coated microneedles for transdermal delivery, J Control Release, 117 (2007) 227-237.
[23] S.L. Thrower, L. James, W. Hall, K.M. Green, S. Arif, J.S. Allen, C. Van-Krinks, B. Lozanoska-Ochser, L. Marquesini, S. Brown, F.S. Wong, C.M. Dayan, M. Peakman, Proinsulin peptide immunotherapy in type 1 diabetes: report of a first-in-man Phase I safety study, Clin Exp Immunol, 155 (2009) 156-165.
[24] Y.C. Kim, F.S. Quan, R.W. Compans, S.M. Kang, M.R. Prausnitz, Formulation of microneedles coated with influenza virus-like particle vaccine, AAPS PharmSciTech, 11 (2010) 1193-1201.
[25] Solubility Guidelines for Peptides (Sigma-Aldrich online rescource), http://www.sigmaaldrich.com/life-science/cell-biology/peptides-and-proteins/peptides-proteins/technical-resource/solubility-guidelines.html.
[26] INSULIN, HUMAN, RECOMBINANT (EXPRESSED IN E. coli) Product information sheet, https://www.sigmaaldrich.com/content/dam/sigma-aldrich/docs/Sigma/Product_Information_Sheet/2/i2767pis.pdf.
[27] S.H. Lipton, C.E. Bodwell, Oxidation of amino acids by dimethyl sulfoxide, Journal of agricultural and food chemistry, 21 (1973) 235-237.
[28] M.A. Fahim, S.A. Al-Muhtaseb, Liquid−Liquid Equilibria of the Ternary System Water + Acetic Acid + 2-Methyl-2-butanol, Journal of Chemical & Engineering Data, 41 (1996) 1311-1314.
[29] A.M. Romgens, D.L. Bader, J.A. Bouwstra, F.P. Baaijens, C.W. Oomens, Monitoring the penetration process of single microneedles with varying tip diameters, J Mech Behav Biomed Mater, 40 (2014) 397-405.
[30] E. Larraneta, J. Moore, E.M. Vicente-Perez, P. Gonzalez-Vazquez, R. Lutton, A.D. Woolfson, R.F. Donnelly, A proposed model membrane and test method for microneedle insertion studies, Int J Pharm, 472 (2014) 65-73.
[31] R.R. Warner, M.C. Myers, D.A. Taylor, Electron probe analysis of human skin: determination of the water concentration profile, J Invest Dermatol, 90 (1988) 218-224.
[32] B. Ghosh, L.H. Reddy, R.V. Kulkarni, J. Khanam, Comparison of skin permeability of drugs in mice and human cadaver skin, Indian journal of experimental biology, 38 (2000) 42-45.
[33] J.R. Bond, B.W. Barry, Limitations of hairless mouse skin as a model for in vitro permeation studies through human skin: hydration damage, J Invest Dermatol, 90 (1988) 486-489.
[34] V.W. Wong, M. Sorkin, J.P. Glotzbach, M.T. Longaker, G.C. Gurtner, Surgical approaches to create murine models of human wound healing, Journal of biomedicine & biotechnology, 2011 (2011) 969618.
[35] M. Kietzmann, D. Lubach, H.J. Heeren, The Mouse Epidermis as a Model in Skin Pharmacology - Influence of Age and Sex on Epidermal Metabolic Reactions and Their Circadian-Rhythms, Lab Anim, 24 (1990) 321-327.

[36] J. Sandby-Moller, T. Poulsen, H.C. Wulf, Epidermal thickness at different body sites: Relationship to age, gender, pigmentation, blood content, skin type and smoking habits, Acta Derm-Venereol, 83 (2003) 410-413.
[37] A. Laurent, F. Mistretta, D. Bottigioli, K. Dahel, C. Goujon, J.F. Nicolas, A. Hennino, P.E. Laurent, Echographic measurement of skin thickness in adults by high frequency ultrasound to assess the appropriate microneedle length for intradermal delivery of vaccines, Vaccine, 25 (2007) 6423-6430.
[38] H.N. Mayrovitz, Assessing Free and Bound Water in Skin at 300 MHz Using Tissue Dielectric Constant Measurements with the MoistureMeterD, in: K.A. Greene, A.S. Slavin, H. Brorson (Eds.) Lymphedema: Presentation, Diagnosis, and Treatment, Springer International Publishing, Cham, 2015, pp. 133-148.
[39] Y.C. Kim, H.E. Grossniklaus, H.F. Edelhauser, M.R. Prausnitz, Intrastromal delivery of bevacizumab using microneedles to treat corneal neovascularization, Invest Ophthalmol Vis Sci, 55 (2014) 7376-7386.

Supplementary Figures:

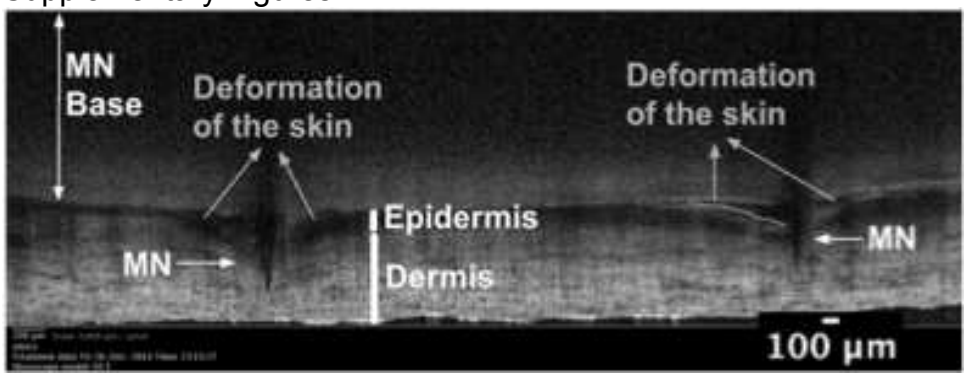

Fig 1. Penetration depth of 500µm length MNs in split-thickness human skin explant.

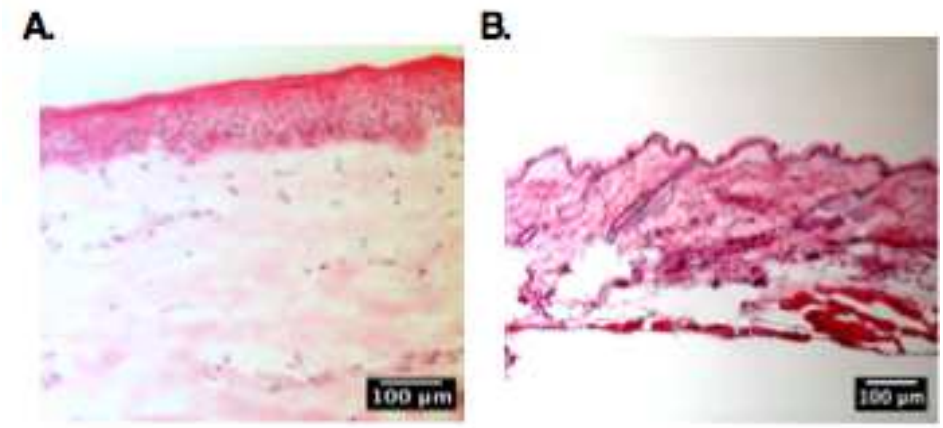

Fig 2. H&E staining of a human and NOD mouse skin section.